INFLUENCE OF DYNAMIC STRAIN AGEING ON DUCTILE FRACTURE OF A C-MN STEEL

H.D. Wang [1,2], C. Berdin [1,3], M. Mazière [4], S. Forest [4], C. Prioul [1], A. Parrot [2]

[1] Laboratoire de Mécanique Sols, Structures et Matériaux, CNRS UMR 8579, Grande Voie des Vignes, 92290 Châtenay-Malabry, France
[2] Electricité de France, R&D Division, Département MMC, Les Renardières, 77818 Moret-sur-Loing, France
[3] Univ. Paris-Sud 11, ICMMO, LEMHE, 91400 Orsay, France
[4] Centre des Matériaux, Mines ParisTech CNRS UMR 7633 BP 87 F-91003 Evry cedex, France

ABSTRACT

Ductile fracture of a C-Mn steel was characterised by tensile tests performed in a large temperature range (from 20 to 350°C) on round notched specimens. The experimental results revealed a sharp drop of fracture strain around 250°C. This corresponds to the domain of dynamic strain ageing (DSA) occurrence. The Portevin-Le Chatelier (PLC) effect, which is the most classical effect of DSA, was modelled on round notched specimens with a mechanical behaviour model including the strain ageing effect. Local approach to fracture was applied to predict the ductile fracture using the Rice and Tracey criterion. The predictions are rather close to the experimental results for the low and high temperatures. In the DSA domain, the approach predicts a decrease of the fracture strain but with a lower magnitude than the experimental one. Therefore, DSA has an effect on mechanical behaviour but also on fracture mechanisms. Consequently, the fracture criterion has to be modified in the presence of DSA.

KEYWORDS

Dynamic strain ageing, ductile fracture, numerical modelling, local approach, Rice and Tracey criterion, strain localisation

1. INTRODUCTION

The DSA effect can occur in many metal alloys within a certain range of temperature and strain rate. This phenomenon is due to the dynamic interaction between solute atoms and mobile dislocations [1]. DSA reduces the strain rate sensitivity of the flow stress and induces a jerky flow when the strain rate sensitivity becomes negative [2]. In such a case, strain localizes into narrow bands associated with stress drops on the stress–strain curve [3]. This is the so-called “Portevin-Le Chatelier (PLC)” effect. DSA is characterised by an increase in flow stress, ultimate tensile strength and a decrease in fracture toughness [4, 5]. Carbon–manganese steels, used for the secondary systems (feed water line and steam line) of pressurized water reactors, are sensitive to DSA at in service temperatures (around 200°C) [4, 5]. Therefore, the design of these components requires the prediction of fracture toughness of these steels in the presence of DSA.

Recently, Wagner et al. [4] proposed to model the ductile fracture of such a C-Mn steel. They used an elastic-plastic constitutive law without considering the DSA effect. To predict the drop in fracture toughness, they applied the Rice and Tracey criterion. So, a critical void growth ratio was identified at each temperature on notched tensile tests results. The results showed a variation in critical void growth ratio, which was not evidenced on fracture surface. Furthermore, DSA can modify the local mechanical variables, especially when strain rate sensitivity is negative: strain localizations occur even in notched specimens.

A constitutive law taking into account DSA is implemented in a finite element code [6, 7]. Thus, the objective of the present study is then to include DSA in the mechanical behaviour and predict with a local approach the fracture of a C-Mn steel in the DSA domain. Consequently, the tensile behaviour is studied and modelled by a law derived from Kubin, McCormick, Estrin's works [2, 8]. The fracture behaviour of a C-Mn steel is characterised with notched tensile tests. Finite element simulations taking into account DSA effect are performed. Finally, the Rice and Tracey [9] criterion is applied to predict the fracture in the presence of DSA.

2. MATERIAL AND EXPERIMENTAL TESTS

The material studied is a Carbon Manganese steel which was presented in the study of Belotteau et al. [5]. Mechanical behaviour of the material was characterised by fourteen tensile tests performed on round tensile specimens at seven temperatures in a large temperature range (20 - 350°C) and at two strain rates: 10^{-2} s^{-1} and $10^{-4}s^{-1}$. The specimens used were round smooth specimens with a gauge length of 36 mm and a diameter of 6 mm. PLC effect was evidenced in the temperature range 150-300°C depending on the prescribed strain rate [5].

Tests on round notched specimens were carried out over the same temperature range. The minimal diameter Φ_0 in the notch section was 10 mm for all samples, but the root notch radius r varied from 2 mm (AE2), 4 mm (AE4) and up to 10 mm (AE10). So, the stress triaxiality that is important for ductile fracture varies between 0.8 to 1.2. The nominal strain rate of 10^{-3} s^{-1} (defined as the mean value of the strain rate in the minimum cross-section) was determined in order to obtain the PLC effect during these tests. Preliminary computations with the finite element method allowed calculating the displacement velocity to be prescribed to the crosshead of testing machine in order to reach the nominal strain rate.

During the tensile tests, the variations of the load P versus diameter Φ, measured at the minimum section, were recorded. From these values, the mean stress $\bar{\sigma} = 4P/\pi\Phi_0^2$ and the mean strain $\bar{\varepsilon} = 2\ln\left(\Phi_0/\Phi\right)^2$ were calculated. The mean stress and strain at failure ($\bar{\sigma}_R$ and $\bar{\varepsilon}_R$ respectively) were determined ($\bar{\sigma}_R$ from final diameter Φ_R measured on broken specimens).

The test results showed that at 200°C, the PLC effect occurred: so, jerky flow behaviour is noted not only on smooth tensile specimen, but also on notched specimen (Fig. 1. a). The largest mean stress (i.e. the largest load) is reached at 350°C, then at 200 and 20°C. This non monotonous evolution is not classical and stems from the overhardening due to solute dragging on dislocations. At 200°C, jerky flow is noted for all geometries (Fig. 1. b). The stress level between AE2 and AE4 is very close whereas stress level of AE10 is much lower. This is due to the PLC effect which is related to strain rate: indeed, the solute drag effect is

function of local strain rate; even if the mean strain rate around the notch is the same in notched specimens (AE2 and AE4), the distribution along the notch radius is different, so the overhardening due to solute dragging is different too. Fig. 2 shows the fracture strain $\overline{\varepsilon}_R$ variation with temperatures for AE2, AE4 and AE10 specimens. A sharp drop of the fracture strain $\overline{\varepsilon}_R$ is evidenced. The decrease of the fracture strain $\overline{\varepsilon}_R$ is less pronounced when the stress triaxiality is higher. Indeed, in the classic case, fracture strain increases with temperature. Fractographic analysis by SEM (Scanning Electron Microscopy) of broken specimens showed no clear evidence of dimple size modification.

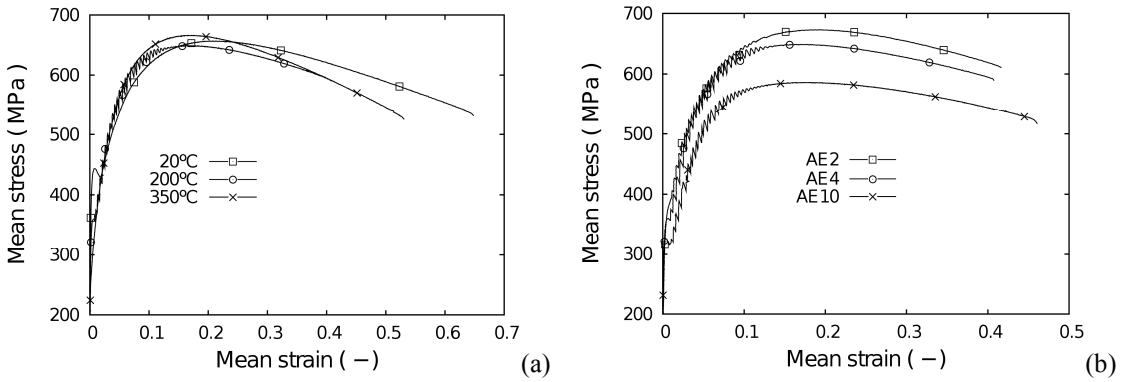

Fig. 1: Mean stress versus mean strain: (a) for AE4 specimens tested at 20°C, 200°C and 350°C (b) AE2, AE4 and AE10 specimens tested at 200°C

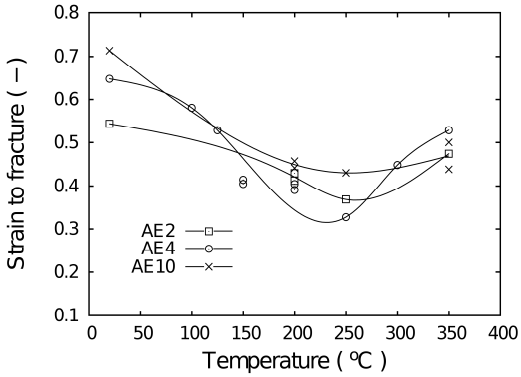

Fig. 2: Strain to fracture for AE2, AE4 and AE10 at 200°C

3. NUMERICAL MODELLING

3.1 Constitutive model

For the modelling of the PLC phenomenon, the KEMC strain ageing model was used. This thermally activated elasto-viscoplastic model, which derived from models proposed by Kubin and Estrin [2] and McCormick [8], allows the prediction of both types of strain ageing: static strain ageing (SSA) (Lüders effect) and DSA (PLC effect). It was first proposed by Zhang et al. [10] and adapted by Graff et al. [6]. In the KEMC model, an internal variable, the ageing time t_a, was introduced to model the overhardening due to strain ageing. Higher values of t_a induce stronger overhardening. The evolution law of the ageing time depends on the plastic strain rate through a parameter ω which represents the strain increment produced when all

arrested dislocations overcome localised obstacles and advance to the next pinned configuration (equation 3). The yield function f is based on the von Mises criterion with isotropic hardening:

$$f\left(\underset{\sim}{\sigma},R,R_a\right)=J_2\left(\underset{\sim}{\sigma}\right)-R-R_a \tag{1}$$

The term $J_2\left(\underset{\sim}{\sigma}\right)$ represents the second invariant of the stress tensor deviator and R is the isotropic strain hardening. The particularity of the KEMC model is the introduction of the term R_a which represents the overhardening due to strain ageing:

$$R_a\left(C_s\right)=P_1C_s \tag{2}$$

where R_a is a function of the variable C_s, defined as the local concentration of solute atoms at temporarily arrested dislocations. The parameter P_1 represents the maximal stress drop magnitude from a fully pinned state to a fully unpinned state. The non-dimensional solute concentration evolves to a saturation value C_m when the ageing time t_a tends to infinity. The variable p is the cumulated equivalent plastic strain. The parameters P_2, α and n are constants:

$$C_s\left(p,t_a\right)=C_m\left(1-exp\left(-P_2p^{\alpha}{t_a}^{n}\right)\right),\ \ \dot{t}_a=1-\frac{\dot{p}}{\omega}t_a,\ \ t_a(t=0)=t_{a0} \tag{3}$$

For more details of the KEMC model, readers are referred to the study of Belotteau et al. [5].

Fig. 3 represents the comparison of numerical and experimental tensile curves for two different temperatures at $10^{-3}s^{-1}$. As can be seen, the KEMC model simulates both strain ageing phenomena: SSA (Lüders stress peak and plateau and Lüders bands) and DSA (serrated flow and PLC bands).

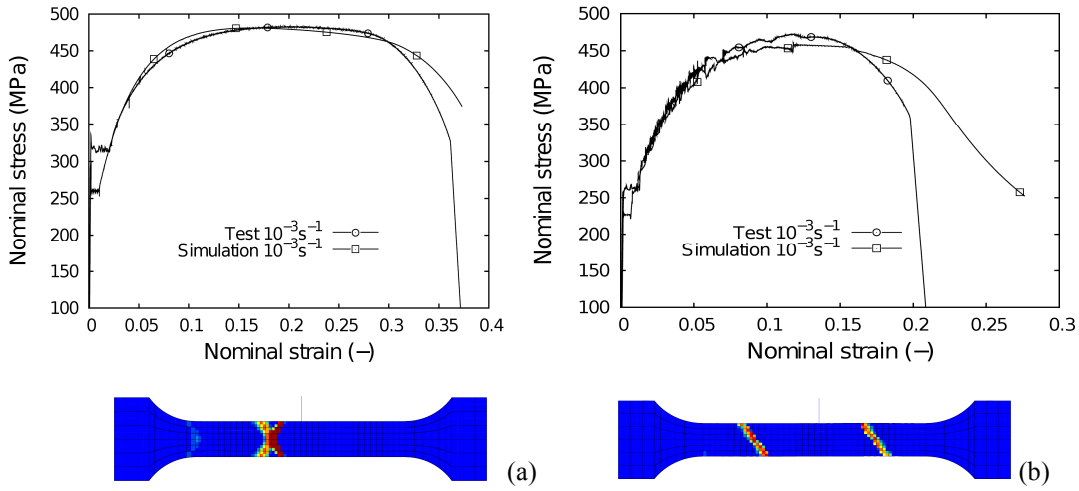

Fig. 3: Numerical and experimental tensile curves for 20°C (a) and 200°C (b) at $10^{-3}s^{-1}$ and the corresponding strain localisation bands (Lüders band (a) and PLC band (b))

3.2 Round notched specimens

The tests on round notched tensile specimens were simulated using the KEMC model which was implemented in a finite element software [6, 7]. 2D-axisymmetric and full 3D computations were performed (Fig. 4). Generally, tensile tests on round notched specimens are modelled in axisymmetric 2D state. However, in the presence of DSA effect, strain

localisation bands could occur and these bands present probably neither axisymmetry nor planar symmetry. Indeed, Graff et al. [6] showed, by in situ observations on polished surfaces of the specimens, that PLC bands on flat U-notched tensile specimens were not symmetric. Therefore, full 3D computations are necessary to correctly predict the DSA effect.

The elements used are eight nodes quadratic elements with reduced integration. The applied boundary conditions were the following (Fig. 4):

1) 2D simulations: displacement equal to zero on the axis of the specimen in direction 1, displacement equal to zero on the minimum section in direction 2, and constant displacement rate on the top of the geometry in direction 2.

2) 3D simulations: displacement equal to zero on the bottom bound in direction 2, displacement of one node on the bottom bound equal to zero in direction 1 and 3, displacement of the second node on the bottom bound equal to zero in direction 1 and constant displacement rate on the top bound in direction 2.

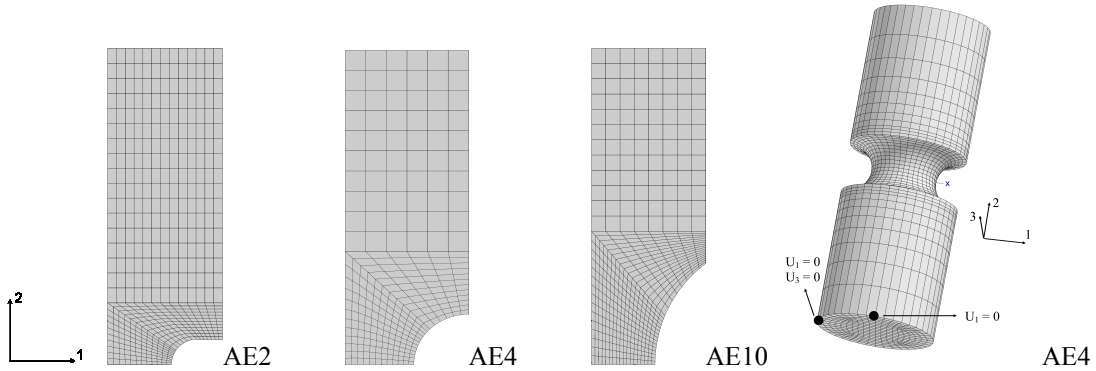

Fig. 4: Mesh geometries for finite element computations

From the tensile curves displayed on Fig. 5 (a), it can be seen that the PLC effect (serrated flow) is correctly predicted by 2D computations on AE specimens tested at 200°C. Fig. 5 (b) displays simulation and experimental results on AE4 in 2D and 3D computations at 200°C.

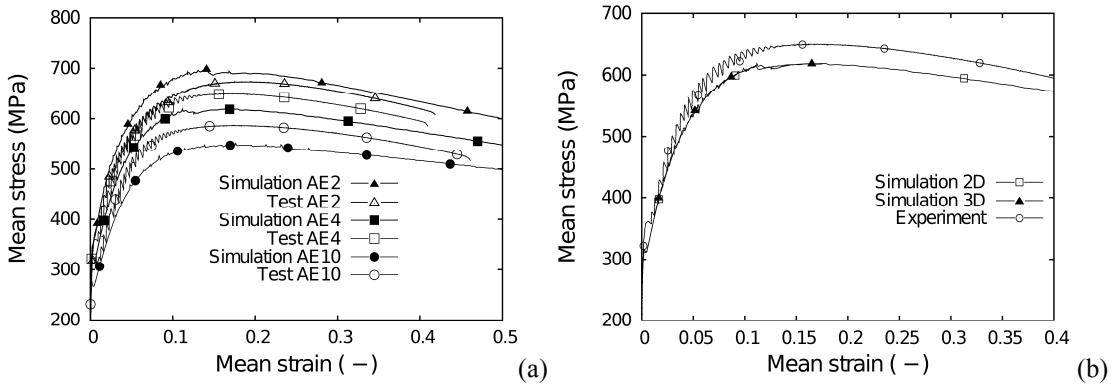

Fig. 5: Mean strain-stress curves at 200°C: (a) tests and 2D simulations for AE2, AE4 and AE10 (b) tests and 2D, 3D simulations for AE4

The results show that the global behaviours predicted by 2D and 3D computations with the KEMC model are identical: they are superposed. However, as can be seen from Fig. 6 and Fig. 7, which display respectively the numerical contour values of equivalent plastic strain

rate for AE2, AE4 and AE10 of 2D computations and for AE4 of 3D computation at 200°C, the characteristics of PLC bands are different in symmetry. Indeed, although PLC bands were observed within the notch and even outside the notch for 2D and 3D simulations, PLC bands on the 3D computation were not axisymmetric (in agreement with the results of Mazière et al. [7]) contrary to the results of 2D simulations. The later were axisymmetric due to the axisymmetric conditions. Consequently, to correctly predict PLC effect on round notched specimens, 3D computations have to be performed.

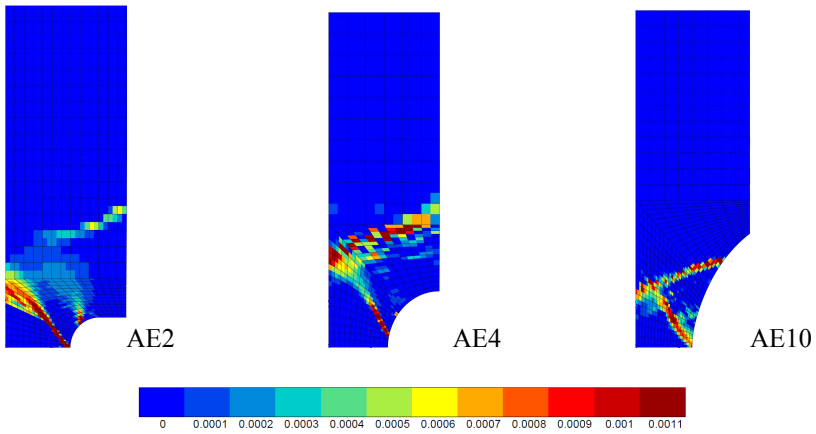

Fig. 6: Contour values of equivalent plastic strain rate of 2D computations at 200°C

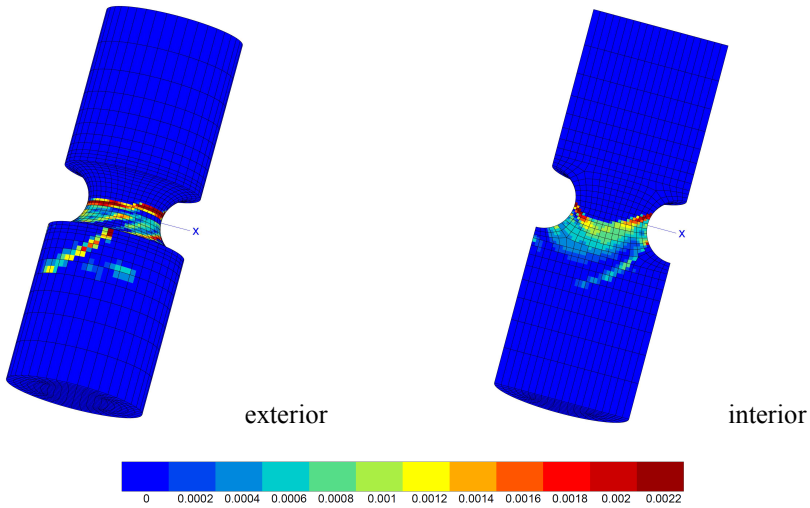

Fig. 7: Contour values of equivalent plastic strain rate for AE4 of 3D computation at 200°C

4. DUCTILE FRACTURE PREDICTION

4.1 Identification of the fracture criterion

The mechanical behaviour of the specimens being correctly simulated, ductile fracture of round notched specimens can then be predicted using the Rice and Tracey model [9]. The void growth ratio is computed at each point of the specimen:

$$\frac{R}{R_0}(t) = \int_0^t \exp\left(\frac{3}{2}\frac{\sigma_m}{\sigma eq}\right)\dot{p}dt \qquad (4)$$

where R is the actual void radius; R_0 is the initial void radius; $\dot{p}$ is the equivalent plastic strain rate; σ_m is the hydrostatic stress; σ_{eq} is the von Mises equivalent stress. Fracture occurs when the void growth ratio reaches a critical value $(R/R_0)_c$. This critical value is identified in order to predict strain to fracture measured in experiments. In the present study, the fracture criterion of Rice and Tracey was supposed to be independent on temperature since the fractographic analysis did not show any particular features on the fracture surfaces of the specimen fractured in the DSA domain. The identification was performed at 20°C through 2D simulations on AE2, AE4 and AE10. Indeed, 2D simulations are sufficient for that purpose because the Rice and Tracey criterion depends on the whole history of the mechanical variables. Although the current variables have not the same value in 2D and in 3D computations as explained before, the integration of the variables over the time does not significantly depend on the symmetry of the model. The criteria identified for each geometry are: 2.31 for AE2, 2.17 for AE4 and 1.88 for AE10. The critical void growth ratio increases slightly with the maximal stress triaxiality ratio occurring in the specimen. This is a classical result since the Rice and Tracey model is more accurate for high stress triaxiality ratio. Therefore, the mean value between AE2 and AE4 (2.24) was taken as the fracture criterion.

4.2 Prediction of ductile fracture

Ductile fracture was predicted on AE4, as displayed on Fig. 8. The decrease observed in the DSA domain is predicted. The predictions at lower and higher temperature were more accurate than those at intermediate temperatures. This may be due to the hypothesis of independence of the criterion on temperature: the criterion probably varies with temperatures due to the DSA effect. Wagner et al. [4] supposed that the criterion was dependent on temperature without justifying this hypothesis. To justify this hypothesis, micromechanical computations on unit cell must be performed.

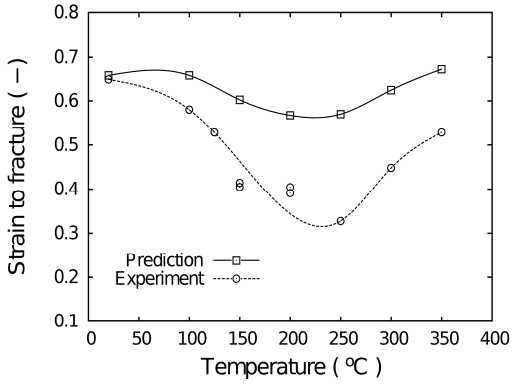

Fig. 8: Prediction of strain to fracture for AE4 from 20°C to 350°C

5. CONCLUDING REMARKS

Tensile tests on round notched specimens were correctly predicted using the KEMC model. 2D and 3D computations showed that full 3D computations were necessary to underline the complicated spatial-temporal characteristics of the PLC instabilities on round notched specimens. Ductile fracture on round notched specimens AE4 at 200°C was correctly predicted using the Rice and Tracey model. However, the prediction for intermediate temperatures was less precise than that for lower and higher temperatures. This could be

explained by the fact that the fracture criterion was modified by the DSA effect at intermediate temperatures: negative strain rate sensitivity probably promotes void coalescence without changing the mechanisms. Therefore, the hypothesis of independence of the fracture criterion on temperature should be modified: the fracture criterion evolves with temperature due to the DSA effect. This point should be justified by micromechanical computations: growth and coalescence of voids under the DSA effect.

REFERENCES

[1] Penning, P.:
Mathematics of the Portevin-Le Chatelier effect
Acta Metall 20 (1972), pp. 1169

[2] Kubin, L.P.; Estrin, Y.:
The Portevin-Le Chatelier effect in deformation with constant stress rate
Acta Metall. 33 (1985), pp. 397-407

[3] Ranc, N.; Wagner, D.:
Some aspects of Portevin-Le Chatelier plastic instabilities investigated by infrared pyrometry
Mat. Sc. Ing. A 394 (2005), pp. 87-95

[4] Wagner, D.; Moreno, J.C.; Prioul, C.; Frund, J.M.; Houssin, B.:
Influence of dynamic strain aging on the ductile tearing of C-Mn steels: modelling by a local approach method
J. Nucl. Mater. 300 (2002), pp. 178-191

[5] Belotteau, J.; Berdin, C.; Forest, S.; Parrot, A.; Prioul, C.:
Mechanical behavior and crack tip plasticity of a strain aging sensitive steel
Mater. Sci. Eng. A 526 (2009), pp. 156-165

[6] Graff, S.; Forest, S.; Strudel, J. -L.; Prioul, C.; Pilvin, P.; Béchade, J. –L.:
Strain Localization phenomena associated with static and dynamic strain ageing in notched specimens : experiments and finite element simulation
Mat. Sci. & Eng., A387-389 (2004), pp. 181-185

[7] Mazière, M.; Besson, J.; Forest, S.; Tanguy, B.; Chalons, H.; Vogel, F.:
Numerical aspects in the finite element simulation of the Portevin – Le Chatelier effect
Comput. Methods Appl. Mech. Engg. 199 (2010), pp. 734-754

[8] McCormick, P.G.:
Theory of flow localisation due to dynamic strain ageing
Acta metall. 36 (1988), pp. 3061-3067

[9] Rice, J.R.; Tracey, D.M.:
On ductile enlargement of voids in triaxial stress fields
J. Mech. Phys. Sol. 17 (1969), pp. 201

[10] Zhang, S.; McCormick, P.G.; Estrin, Y.:
The morphology of Portevin – Le Châtelier bands : finite elements simulations for Al-Mg-Si
Acta Mater. 49 (2001), pp. 1087-1094

Corresponding author: huaidong.wang@ecp.fr